PROCEEDINGS OF SCIENCE

Electroweak Physics at the LHC – Experimental Overview

Philip Sommer* **on behalf of the ATLAS, CMS and LHCb Collaborations**

Technische Universität Dresden

E-mail: philip.sommer@cern.ch

At the LHC, the electroweak theory of the Standard Model of particle physics can be probed through either precision measurements of W and Z boson production or through gauge-boson self-interactions at high energy in multiboson processes. In these proceedings, recent measurements of the fundamental parameters of the electroweak theory, the coupling of the electroweak gauge bosons to fermions and measurements of multiboson production by the ATLAS, CMS and LHCb collaborations are summarised. Many of these measurements exceed the precision achieved at previous collider experiments and significantly extend the energy reach.

42nd International Conference on High Energy Physics (ICHEP2024)
18-24 July 2024
Prague, Czech Republic

*Speaker

PoS(ICHEP2024)031

1. Introduction

In the electroweak theory of the Standard Model of particle physics, the interactions of elementary particles are derived by postulating an $SU(2)_L \times U(1)_Y$ gauge symmetry. This symmetry is broken by the Brout-Englert-Higgs mechanism, resulting in the electroweak gauge bosons, $W^{\pm}$, Z and photon, as the mediators of the electroweak force. All couplings, properties and dynamics of the electroweak gauge bosons are predicted precisely with four fundamental parameters. For example, the theory relates the masses of the $W^{\pm}$ and Z bosons through the weak mixing angle, $\sin\theta_W$.

In pp collision at the LHC [1], the electroweak gauge bosons are produced in the tens of billions. The ATLAS [2], CMS [3] and LHCb [4] experiments have measured their production cross sections over a wide range of centre-of-mass energies. These measurements can be extraordinarily precise and at $\sqrt{s} = 5$ TeV and $\sqrt{s} = 13$ TeV reach a precision of up to 1-2% [5, 6]. As a standard candle, they have also been measured in pp data from the LHC run-3 at $\sqrt{s} = 13.6$ TeV [7, 8]. The measurements are in excellent agreement with theoretical calculations of very high perturbative accuracy. The combination of high events yields and precision in measurements and theoretical calculations allow for stringent experimental tests of the electroweak theory, either at the electroweak mass scale in events where single electroweak gauge bosons are produced or at high energy in the production of multiple electroweak gauge bosons.

2. Fundamental Parameters

The electroweak theory relates the masses of the W and Z bosons, m_W and m_Z, through the electroweak mixing angle, $\sin\theta_W$. Radiative corrections, particularly from the Higgs boson and the top quark, modify the W and Z propagators and decay vertices and, hence, the measurable quantities. For the mass of the W boson, their effect is approximately 1% but measurements target a precision 40 times better than that. Through radiative corrections, measurements of m_W, m_Z and $\sin\theta_W$ are sensitive to a wide range of physics effects. In particular, beyond-the-Standard-Model particles could modify the relation predicted in the electroweak theory.

The ATLAS Collaboration has performed a new measurement of the W boson mass and the first measurement of the W boson width, Γ_W, at the LHC [9]. The W boson mass is measured in $W \to \ell\nu$ decays from the transverse momentum distribution of the lepton, p_{T}^{ℓ}, and the distribution of the transverse mass, m_{T}^{W}. Modifications of the W boson mass within the aspired precision of the measurement change these distributions at the level of a few per-mille and a measurement requires a detailed understanding of the detector response and the theoretical modelling of W boson production. The measurements are based on 4.6 fb^{-1} of pp data collected in 2011 at $\sqrt{s} = 7$ TeV and supersede a previous measurement of m_W using the same dataset [10]. Rigorous checks of the modelling of the transverse momentum distribution of the W boson, p_{T}^{W}, have been performed in data collected in dedicated LHC runs with reduced instantaneous luminosities, offering favourable experimental conditions for the reconstruction of the recoil of the W boson against the protons [5]. Together with progress in global fits of parton distribution functions (PDFs) and theoretical calculations, this allows the measurement of the W boson mass in a profile likelihood fit where data can be used to

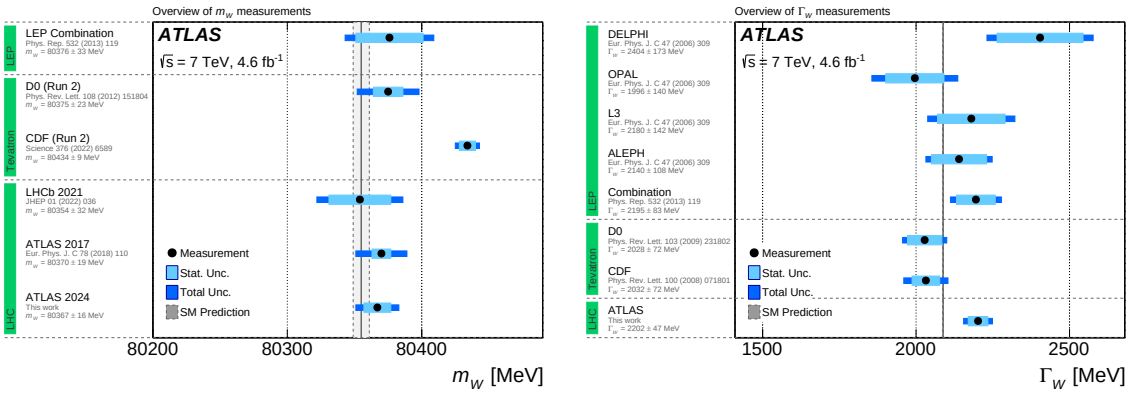

(a) **(b)**

Figure 1: (a) The measured value of the W boson mass, m_W [9]. (b) The measured value of the W boson width, Γ_W [9]. For comparison, the theoretical prediction from the electroweak theory and the measurements from LEP, the Tevatron and previous LHC results are included.

constrain systematic uncertainties. The W boson mass and width are measured to be:

$$m_W = 80366.5 \pm 15.9 \text{ MeV}$$
$$\Gamma_W = 2202 \pm 47 \text{ MeV}.$$

The measurement of the W boson mass is improved by 30% compared to the previous measurement and in agreement with the prediction from the electroweak theory, as well as an earlier measurement by the LHCb collaboration [11]. The W boson width is measured for the first time at the LHC and compatible within two standard deviations with the electroweak theory. It is the most precise measurement from a single experiment. A comparison of the values measured at various experiments and the theoretical prediction from the electroweak theory are shown in Figure 1.

The CMS and LHCb collaborations have performed measurements of the effective leptonic electroweak mixing angle, $\sin^2\theta^\ell_{\text{eff}}$, in $Z \to \ell\ell$ decays in pp collision data from the LHC run-2 [12, 13]. Compared to $\sin\theta_W$, the measured quantity $\sin^2\theta^\ell_{\text{eff}}$ includes the aforementioned radiative corrections to the Z boson decay vertex. The interference of vector and axial-vector neutral currents introduces an asymmetry in the scattering of a valence quark and an anti–sea-quark. Ambiguities in the quark direction are resolved through a rapidity-dependent measurement of the asymmetry, shown in Figure 2a. Kinematic access to large values of rapidity is therefore beneficial to the measurement. The acceptance of the track reconstruction in the CMS detector restricts the acceptance for muons to $|y_{\ell\ell}| < 2.4$. By combining electrons reconstructed in the acceptance of the tracking detectors with a reconstructed calorimeter cluster in the forward calorimeters, the acceptance is significantly extended to $|y_{\ell\ell}| < 4.36$. A comparison of the values of $\sin^2\theta^\ell_{\text{eff}}$ measured in various channels, as well as their stability in different datasets, is shown in Figure 2b. The interplay of events with low and high rapidity allows constraining uncertainties in the PDFs of which several global combinations are compared to the measurement. In addition to a reduced sensitivity to PDF uncertainties, the spread of the measurement from several global PDF sets is reduced as well. Both effects are demonstrated in Figure 2c. The PDFs remain the dominant

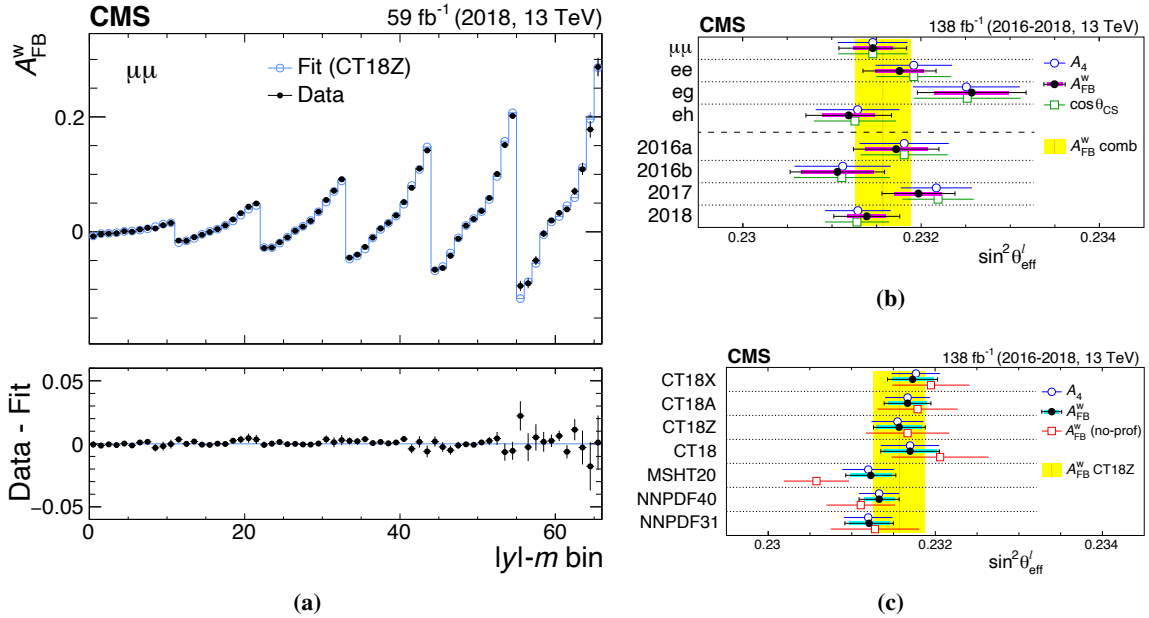

Figure 2: (a) Measured asymmetry as a function of $y_{\ell\ell}$ and $m_{\ell\ell}$. The effective leptonic electroweak mixing angle, $\sin^2\theta_{\text{eff}}$, is extracted in a fit of this distribution, the result of which is shown as well [12]. (b) Measured values of $\sin^2\theta_{\text{eff}}$ obtained in various Z boson decay channels and in different datasets [12]. (c) Measured values of $\sin^2\theta_{\text{eff}}$ for different choices of global PDF sets [12].

source of uncertainty. The measurement from the LHCb Collaboration benefits from precision muon reconstruction in the range $2.0 < |y_{\ell\ell}| < 4.5$. In this kinematic range, PDF uncertainties are generally smaller. The measurement is, however, statistically limited since the LHCb experiment runs with lower instantaneous luminosities compared to the CMS experiment, resulting in a dataset of 5.3 fb^{-1} compared to 138 fb^{-1} for the LHC run-2. The effective leptonic electroweak mixing angle is measured to be:

$$\begin{aligned}\text{CMS:}\ \sin^2\theta^{\ell}_{\text{eff}} &= 0.23157 \pm 0.00010\,(\text{stat}) \pm 0.00015\,(\text{syst}) \pm 0.00009\,(\text{theo}) \pm 0.00027\,(\text{PDF})\\ \text{LHCb:}\ \sin^2\theta^{\ell}_{\text{eff}} &= 0.23152 \pm 0.00044\,(\text{stat}) \pm 0.00005\,(\text{syst}) \pm 0.00022\,(\text{theo/PDF}).\end{aligned}$$

The theoretical prediction is in agreement with the measurements. The measurement by the CMS Collaboration improves on previous measurements at the Tevatron and LHC [14].

3. Electroweak Coupling of Fermions

Measurements of the branching fraction of on-shell W bosons have traditionally relied on ratio measurements of different decay modes in W boson pair production. At the LHC, W boson pairs are most prevalent in the decay of top quark pairs that can be selected with high purity using the displacement of the decay vertices of b-quark jets produced in the top decay.

The ATLAS Collaboration has performed measurements of electron-muon universality of on-shell W boson decays by forming ratios of $WW \to e\nu\mu\nu$, $e\nu e\nu$ and $\mu\nu\mu\nu$ decays [15]. The measurement is based on events from top quark pair production selected in 140 fb^{-1} of pp data. To

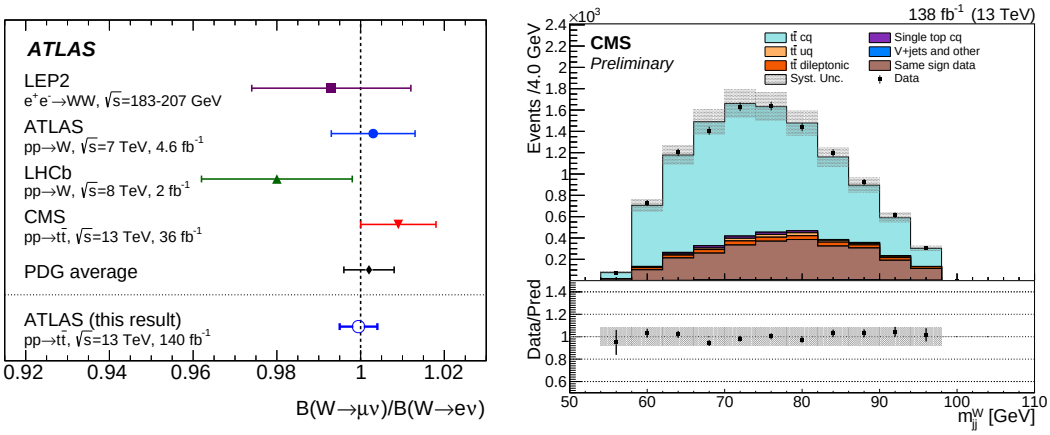

(a) **(b)**

Figure 3: (a) Measured relative $W \to \mu\nu/W \to e\nu$ branching ratio for on-shell W bosons produced in the decay of top quark pairs [15]. Several previous measurements and the current world average are compared to the measurement. (b) Invariant mass distribution of two jets from a $W \to cq$ decay [19]. The presence of a charm quark is identified through its decay to a muon which is reconstructed inside the jet.

reduce the size of systematic uncertainties in the electron and muon reconstruction, the branching ratios are measured relative to the $Z \to ee$ and $\mu\mu$ branching ratios in ATLAS and at LEP which are known much more precisely than those of W boson decays. The measurement is consistent with and improves on the current world average [16]. It complements earlier measurement of electron–τ-lepton universality by ATLAS [17] and a similar measurement by the CMS Collaboration [18].

The CMS Collaboration has measured the ratio of $W \to cq$ and $W \to qq$ branching fractions of the W boson in top quark pair events selected in 138 fb^{-1} of data [19]. The measurement is facilitated by reconstructing muons from charm-quark decays, i.e. by the presence of a muon inside of a jet. The signal purity of the selected events is very high, as shown in Figure 3b. The relative branching ratio to charm quarks is measured to be 0.489 ± 0.020, consistent with the electroweak theory and dramatically improving the precision of previous measurements. The results are interpreted to determine V_{cs} by assuming the unitarity of the CKM matrix. The measurement of V_{cs} is competitive with earlier measurements at the LHC from the W and Z boson production cross section ratio [20].

The production of a pair of τ leptons from photons proceeds through purely electromagnetic interactions and is sensitive to the anomalous magnetic and electric dipole moments of the τ lepton. It has been measured by the CMS Collaboration [21]. The protons remain intact in the interactions or fragment in the forward direction, outside of the acceptance of the CMS tracking detectors. The key experimental signature is the absence of any charged particles in the vicinity of the primary interaction vertex other than those produced in the decay of the τ lepton. The interpretation of the measurement dramatically improves previous constraints on the τ anomalous magnetic moment from τ-lepton pairs produced in ultra-peripheral heavy-ion collision [22, 23] since pp collisions have a higher energy reach. In fact, the energy is large enough to produce particles at the electroweak scale and the same experimental techniques have allowed the ATLAS Collaboration to observe the

production of W boson pairs from photons [24].

4. Electroweak Gauge Sector

Tests of the electroweak theory at high energy proceed through processes producing multiple electroweak gauge bosons. Characteristic for these processes is that they involve interactions amongst the gauge bosons themselves. Individual diagrams typically diverge with energy, but those divergences are cancelled through the interplay of multiple diagrams. Any beyond-the-Standard Model contributions, however, would destroy the exact cancellations leading to potentially very large effects.

Measurements of diboson production now routinely reach a precision of 5% or better. The production of two massive electroweak gauge bosons, WW, ZZ and WZ, have been measured at the LHC for various centre-of-mass energies, most recently in LHC run-3 data from 2022 at $\sqrt{s}$ = 13.6 TeV [25–27]. The progress over the last years in both the experimental techniques and in calculations from theory is best illustrated in the measurement of $pp \to WW$ production. The measurement is now routinely performed in a jet-inclusive phase space, reducing both the experimental and the theoretical uncertainties in the measurement. The theoretical prediction at next-to-next-to-leading order, interfaced to parton showers, is in excellent agreement with the differential measurement of the jet multiplicity.

While diboson production can proceed through trilinear gauge couplings, the production of three electroweak gauge bosons and the scattering of two electroweak gauge bosons can proceed through quartic electroweak self interactions. These are amongst the rarest processes experimentally accessible at the LHC. The large datasets of the LHC run-2, amounting to 140 fb^{-1} in ATLAS and 138 fb^{-1} in CMS, allowed for the observation of vector-boson scattering in all major decay channels. The measurements exploit the characteristic signature: two electroweak gauge bosons are radiated off of two quarks and proceed to scatter. Since no colour charge is exchanged between the two quarks, they fragment in the forward direction with large rapidity separation. Triboson production, on the other hand, is experimentally more challenging and does not yet reach the same precision as vector-boson scattering.

Recent examples of measurements involving quartic electroweak couplings are measurements of purely electroweak $W\gamma jj$ production by the ATLAS Collaboration [28], a process sensitive to $W\gamma$ scattering, and $WZ\gamma$ production [29] by the CMS Collaboration. The scattering of electroweak gauge bosons to a $W\gamma$ pair is observed with more than six standard deviations using a fit to a neural-network discriminant that exploits the characteristic vector-boson scattering signature. Differential distributions are measured as well and do not rely on multivariate discriminants, therefore reducing the theoretical assumptions in the measurement. The measured dijet invariant mass distribution is shown in Figure 4a. The $WZ\gamma$ production is observed with a significance of 5.4 standard deviations from a fit to the $Z\gamma$ invariant mass, $m_{Z\gamma}$, shown in Figure 4b. Both processes had been observed previously by the CMS [30] and ATLAS [31] experiments.

The agreement of the data with the electroweak theory is quantified by constraining higher-dimensional operators built from the Standard Model fields in an Effective Field Theory expansion. In the Standard Model Effective Field Theory, operators affecting quartic electroweak couplings only enter at dimension-8. Interpretations in Effective Field Theories are routinely performed in

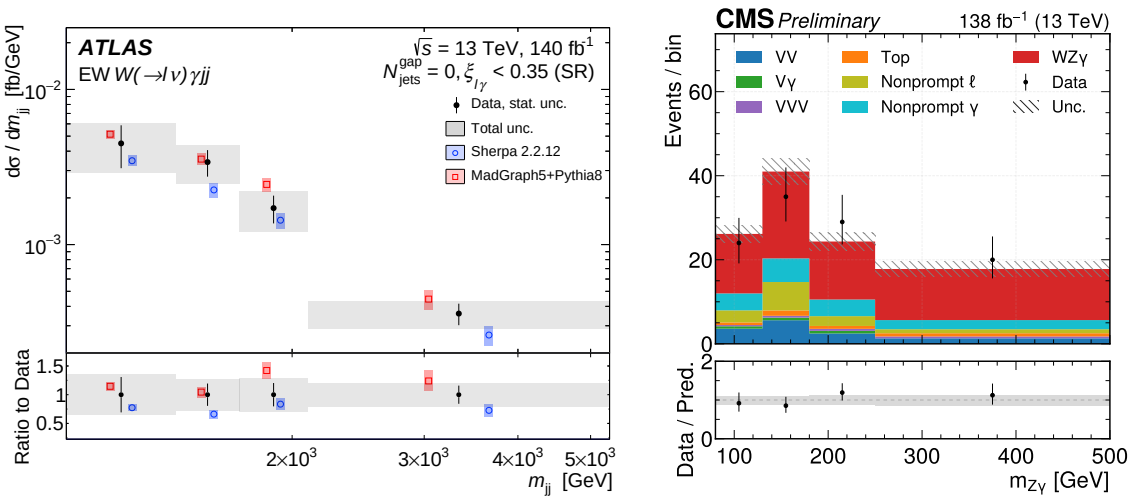

(a) **(b)**

Figure 4: (a) Measured dijet invariant mass, m_{jj}, in $W\gamma$ scattering. Theoretical predictions from state-of-the-art event generators are compared to the measurement [28]. (b) Distribution of the $Z\gamma$ invariant mass, $m_{Z\gamma}$, in the measurement of $WZ\gamma$ production. The observation is reported from a fit to $m_{Z\gamma}$ [29].

measurements of triboson production and vector-boson scattering. Limits on dimension-8 operators are usually provided as a function of an upper bound of the diboson mass imposed on the simulated Effective Field Theory contributions. The partial-wave unitarity of these contributions is ensured by comparing the mass-dependent constraints with theoretical bounds. The experimental sensitivity in the data from the LHC run-2 is for the first time sufficient to provide unitarised limits on operators built solely from covariant derivatives of the Higgs field [32], indicating that measurements of vector-boson scattering become sensitive to electroweak symmetry breaking via the Brout-Englert-Higgs mechanism.

Other studies of electroweak symmetry breaking measure the polarisation of the electroweak gauge bosons in diboson production. In the electroweak theory, the longitudinal polarisation states of the W and Z bosons are generated by absorbing three of the four degrees of freedom introduced by the Higgs field. Asymptotically, they behave like the original components of the Higgs field. The polarisation is reconstructed from the angular distributions of the decay products of W and Z bosons. The measurements rely on a decomposition of diboson production cross sections into double-longitudinal, mixed longitudinal–transverse and double-transverse components. The joint polarisation of a WZ boson pair has been observed by the ATLAS Collaboration [34], measuring the three polarisation components individually by categorising events according to the decay angles of the two gauge boson decay products, and further separating the decay products with a neural-network classifier.

More recently, evidence for the joint diboson polarisation was obtained in ZZ production [35]. In WZ production, the energy dependence of the polarisation fractions was studied as a function of the transverse momentum of the Z boson [36]. Both measurements extract the double-longitudinal component through a fit of a boosted-decision tree discriminant, shown in Figures 5, to separate it

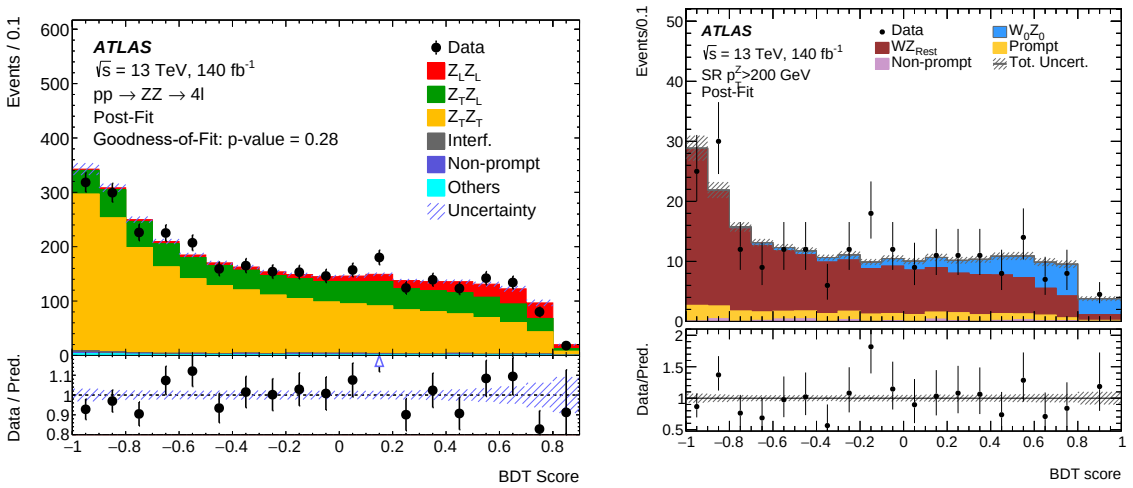

(a) **(b)**

Figure 5: Distributions of the boosted-decision tree discriminant in data and simulated events. They are shown (a) for the measurement of double-longitudinal ZZ production [35] and (b) for double-longitudinal WZ production in a phase space selected with $p_{\mathrm{T}}^{Z} > 200$ GeV [36]. The uncertainty bands in the simulated events include the statistical and systematic uncertainties as obtained in the fit.

from other polarisation components. An important measurement for the future will be the scattering of longitudinally polarised W bosons which has already been studied by the CMS Collaboration in data from the LHC run-2 [38].

5. Summary

The ATLAS, CMS and LHCb experiments have recently performed numerous precise tests of the electroweak theory, that in many areas are competitive or exceeding the precision of previous particle collider experiments. The high precision is facilitated by the large datasets delivered by the LHC and a detailed understanding of the detectors. A key component is the use of dedicated reconstruction techniques and the use of state-of-the-art theoretical calculations.

Novel measurements of two fundamental parameters of the electroweak theory, the W boson mass and the effective leptonic electroweak mixing angle, have been performed. The coupling of leptons to on-shell W bosons has been tested with unprecedented precision. At the same time, the electroweak theory has been tested at highest energy in multiboson measurements, in particular in vector-boson scattering processes and triboson production. Moreover, measurements of the polarisation of the gauge bosons in diboson production have been performed. These measurements join dedicated measurements on the Higgs boson resonance in improving our understanding of electroweak symmetry breaking through the Brout-Englert-Higgs mechanism.

References

[1] L. Evans and P. Bryant, JINST **3** (2008) S08001.

[2] ATLAS Collaboration, JINST **3** (2008) S08003.

[3] CMS Collaboration, JINST **3** (2008) S08004.

[4] LHCb Collaboration, JINST **3** (2008) S08005.

[5] ATLAS Collaboration, arXiv:2404.06204 [hep-ex].

[6] CMS Collaboration, arXiv:2408.03744 [hep-ex].

[7] ATLAS Collaboration, Phys. Lett. B **854** (2024) 138725.

[8] CMS Collaboration, CMS-PAS-SMP-22-017.

[9] ATLAS Collaboration, arXiv:2403.15085 [hep-ex].

[10] ATLAS Collaboration, Eur. Phys. J. C **78** (2018) 110.

[11] LHCb Collaboration, JHEP **01** (2022) 036.

[12] CMS Collaboration, arXiv:2408.07622 [hep-ex].

[13] LHCb Collaboration, to be published.

[14] ATLAS Collaboration, ATLAS-CONF-2018-037.

[15] ATLAS Collaboration, arXiv:2403.02133 [hep-ex].

[16] Particle Data Group, PTEP **2022** (2022) 083C01.

[17] ATLAS Collaboration, Nature Phys. **17** (2021) 813-818.

[18] CMS Collaboration, Phys. Rev. D **105** (2022) 072008.

[19] CMS Collaboration, CMS-PAS-SMP-24-009.

[20] ATLAS Collaboration, Eur. Phys. J. C **77** (2017) 367.

[21] CMS Collaboration, Rept. Prog. Phys. **87** (2024) 107801.

[22] ATLAS Collaboration, Phys. Rev. Lett. **131** (2023) 151802.

[23] CMS Collaboration, Phys. Rev. Lett. **131** (2023) 151803.

[24] ATLAS Collaboration, Phys. Lett. B **816** (2021) 136190.

[25] CMS Collaboration, arXiv:2406.05101 [hep-ex].

[26] ATLAS Collaboration, Phys. Lett. B **855** (2024) 138764.

[27] CMS Collaboration, CMS-PAS-SMP-24-005.

[28] ATLAS Collaboration, arXiv:2403.02809 [hep-ex].

[29] CMS Collaboration, CMS-PAS-SMP-22-018.

[30] CMS Collaboration, Phys. Rev. D **108** (2023) 032017.

[31] ATLAS Collaboration, Phys. Rev. Lett. **132** (2024) 021802.

[32] ATLAS Collaboration, JHEP **06** (2024) 192.

[33] CMS Collaboration, CMS-PAS-SMP-22-008.

[34] ATLAS Collaboration, Phys. Lett. B **843** (2023) 137895.

[35] ATLAS Collaboration, JHEP **12** (2023) 107.

[36] ATLAS Collaboration, Phys. Rev. Lett. **133** (2024) 101802.

[37] https://atlas.web.cern.ch/Atlas/GROUPS/PHYSICS/PAPERS/STDM-2020-01/

[38] CMS Collaboration, Phys. Lett. B **812** (2021) 136018.